Dynamics and physical interpretation of quasistationary states in systems with long-range interactions

T. M. Rocha Filho, M. A. Amato, A. E. Santana, and A. Figueiredo
Instituto de Física and International Center for Condensed Matter Physics Universidade de Brasília, CP 04455, 70919-970 Brasília, Brazil

J. R. Steiner
Instituto de Física, Universidade de Brasília, CP 04455, 70919-970 Brasília, Brazil

(Received 13 May 2013; revised manuscript received 23 July 2013; published 13 March 2014)

The time evolution of the one-particle distribution function of an N-particle classical Hamiltonian system with long-range interactions satisfies the Vlasov equation in the limit of infinite N. In this paper we present a new derivation of this result using a different approach allowing a discussion of the role of interparticle correlations on the system dynamics. Otherwise for finite N collisional corrections must be introduced. This has allowed a quite comprehensive study of the quasistationary states (QSSs) though many aspects of the physical interpretations of these states still remain unclear. In this paper a proper definition of time scale for long time evolution is discussed, and several numerical results are presented for different values of N. Previous reports indicate that the lifetimes of the QSS scale as $N^{1.7}$ or even the system properties scale with $\exp(N)$. However, preliminary results presented here indicates that time scale goes as N^2 for a different type of initial condition. We also discuss how the form of the interparticle potential determines the convergence of the N-particle dynamics to the Vlasov equation. The results are obtained in the context of the following models: the Hamiltonian mean field, the Self-gravitating ring model, and one- and two-dimensional systems of gravitating particles. We have also provided information of the validity of the Vlasov equation for finite N.

DOI: 10.1103/PhysRevE.89.032116 PACS number(s): 05.20.Dd, 05.10.Gg

I. INTRODUCTION

Long-range interacting systems are characterized by an interaction potential decaying at long distances as $r^{-\alpha}$ such that $\alpha < d$, with d being the space dimension. This may lead to anomalous behavior such as non-Gaussian quasi-stationary states (QSSs), negative (microcanonical) heat capacity, ensemble inequivalence, and nonergodicity [1–6]. Examples of systems with long-range interactions include self-gravitating systems (stars in galaxies and globular clusters), non-neutral plasmas, and two-dimensional vortices [7–15]. The existence of nonequilibrium non-Gaussian QSSs have been explained by identifying them with stationary states of the Vlasov equation [1,16], which describes the dynamics of the statistical states of such systems. We write the Hamiltonian of an N-particle classical system with long-range interactions as

$$H = \sum_{i=1}^{N} \frac{\mathbf{p}_i^2}{2m} + \frac{1}{N} \sum_{i<j=1}^{N} V_{ij}, \tag{1}$$

with $V_{ij} \equiv V(|\mathbf{r}_i - \mathbf{r}_j|)$ and $\mathbf{r}_i$, $\mathbf{p}_i$ are the position and momentum vectors for particle i, respectively, and m the mass of the identical particles. The Kac factor $1/N$ in the potential energy term in Eq. (1) is introduced such that the total energy is extensive [17]. In a seminal and quite intricate paper [18] Braun and Hepp showed that the time evolution of the one-particle distribution function $f(\mathbf{r},\mathbf{p},t)$ for those systems satisfies the Vlasov equation in the limit $N \to \infty$:

$$\frac{\partial f}{\partial t} + \frac{\mathbf{p}}{m} \cdot \frac{\partial f}{\partial \mathbf{r}} + \mathbf{F} \cdot \frac{\partial f}{\partial \mathbf{p}} = 0, \tag{2}$$

where the mean-field force and potential are given, respectively, by

$$\mathbf{F}(\mathbf{r},t) = -\frac{\partial}{\partial \mathbf{r}} \overline{V}(\mathbf{r},t),$$
$$\overline{V}(\mathbf{r},t) = \int v(\mathbf{r}-\mathbf{r}') f(\mathbf{r}',\mathbf{p}',t)\, d\mathbf{p}'\, d\mathbf{r}'. \tag{3}$$

For finite N Eq. (2) is valid only up to terms $O(N^{-1})$, and collisional corrections become relevant (see Ref. [1] and references therein). The property of vanishing interparticle correlations in the initial state is consistently propagated by the Hamiltonian dynamics in the $N \to \infty$ limit. For practical purposes, the Vlasov equation is used as a good approximation for sufficiently large N, its validity being limited to short times. Although the lifetime of QSSs has been extensively studied in the literature [19–27] many aspects of its physical interpretation and phenomenology remain unclear. In the present paper we discuss how to define properly a time scale for its long-time evolution, which is governed by collisional corrections to the Vlasov equation leading to the Landau or Balescu-Lenard kinetic equations (see Refs. [28–31] and references therein). For homogeneous one-dimensional systems the collision terms of both Landau and Balescu-Lenard equations vanish identically [28,32] and higher order corrections must be considered in the kinetic equations, leading to an evolution time scale of order N^{δ} with $\delta > 1$ for homogeneous and of order N for inhomogeneous states. For the Hamiltonian mean field (HMF) model (see Sec. III) a value of $\delta = 1.7$ was claimed by Yamaguchi *et al.* [33] and by Bouchet and Dauxois [34] for a homogeneous water-bag initial condition, while Campa *et al.* [20] and Chavanis [35] have reported a time scale of order $\exp(N)$ for a semielliptic initial homogeneous state. This is to be compared to a time scale of order N^2 estimated

numerically for one-dimensional plasmas [36,37] and to the same scaling for the dynamics of a three-level homogeneous initial state for the HMF model presented in Sec. V. Also, as we argue below, for most of the QSS a lifetime cannot be defined consistently. In such cases it must be replaced by the notion of a characteristic time scale (relaxation time).

We also study the scope of validity of the Vlasov equation for finite N and for some representative models with long-range interactions, i.e., how the dynamics converges to the mean-field (Vlasov) description as N increases and how interparticle correlations arise and how the dynamics depends on them. The representative models referred to are the Hamiltonian mean field (HMF) model [38], the self-gravitating ring model [14], and one- and two-dimensional self-gravitating particles [8,39]. There are a few approaches to deduce the Vlasov equation from first principles for long-range forces [1,18,40]. Here we choose the one by Balescu, which allows an explicit estimation of the order of magnitude of many contributions, and most importantly, that of interparticle correlations [41,42]. The Vlasov and Balescu-Lenard equations were previously obtained by Balescu using the plasma constant as a (small) parameter in the diagrammatic representation of the series solution. Here we show that the Kac factor fulfills a similar role. For sake of completeness and for the present paper to be self-contained, we present this approach in the appendices. It is shown that provided all interparticle correlations are dynamically created, they do not alter the validity of the Vlasov equation. This means that deviations from the solution of the Vlasov equation are not due to the creation of correlations with time (even though they are always present), since their order of magnitude is preserved by the dynamics, but to the secular accumulation of small collisional corrections of order $1/N$ (see Sec. IV). The one-particle distribution function at any point of the evolution can thus be used as the initial condition to solve the Vlasov equation, which is valid for a given time span starting at this value of time. This is important for the interpretation of the QSSs and their characteristic lifetimes.

This paper is structured in the following way: Sec. II presents the deduction of the Vlasov equation from Balescu's dynamics of correlations approach. In Sec. III we discuss the effect of the explicit form of the interparticle potential on the convergence of the N-particle dynamics to the solution of the Vlasov equation. Sec. IV discusses the behavior of interparticle correlation with time from simulation data and Sec. V the physical interpretation of quasistationary states in the light of previous sections. We close the paper with some concluding remarks in Sec. VI. In Appendix A we briefly present the dynamics of correlations formalism of Balescu, and in Appendix B we discuss how it can be extended for self-gravitating systems with different masses.

II. DYNAMICS OF CORRELATIONS AND THE VLASOV EQUATION

The diagrammatic approach for the solution of the N-particle Liouville equation was used by Balescu to deduce the Vlasov equation for plasmas as a lower order evolution equation in the plasma parameter [41,42]. In this section we show that the Kac factor $1/N$ in the interaction potential leads naturally to the Vlasov equation by allowing us to select the diagrams contributing to the solution of the Liouville equation [41]. We believe that the present approach is more physically appealing and allows us to assess explicitly the different relevant contributions to the Vlasov equation.

We consider here a system of identical particles with unit masses $m = 1$ and the Hamiltonian in Eq. (1) with Cartesian coordinates where $V_{ij} \equiv V(|\mathbf{r}_i - \mathbf{r}_j|)$ is the pair interaction potential for particles i and j, $\mathbf{r}_i$ denotes the position of particle i, and $\mathbf{v}_i$ its velocity. Thus in all that follows we have $\mathbf{p}_i = \mathbf{v}_i$. Formally going from a probability density as a function of the momenta to one written as a function of the velocities involves a change of unit, but due to the choice $m = 1$ both are equal up to a trivial multiplication by a constant equal to one times the unit of mass. This equality is considered implicitly were required. The probability that particle i is in the phase volume $d\mathbf{r}_i d\mathbf{v}_i$ for $i = 1, \ldots, N$ is written as (we use the notation of Ref. [16])

$$f_N(1,2,\ldots,N)\, d1\, d2 \cdots dN, \tag{4}$$

where f_N is the N-particle distribution function, and we write 1 for $\mathbf{r}_1, \mathbf{v}_1$, $d1 \equiv d\mathbf{r}_1 d\mathbf{v}_1$, 2 for $\mathbf{r}_2, \mathbf{v}_2$, $d2 \equiv d\mathbf{r}_2 d\mathbf{v}_2$, and so on. We impose that f_N is a symmetric function with respect to particle interchange.The s-particle distribution function is defined by

$$f_s(1,\ldots,s) = \int f_N(1,\ldots,N)\, d(s+1) \cdots dN. \tag{5}$$

For a closed system f_N satisfies the Liouville equation:

$$i \frac{\partial f_N}{\partial t} = \hat{L}_N f_N, \tag{6}$$

with the Liouville operator given by

$$\hat{L}_N \equiv i\,\{H,\} = i \sum_{i=1}^{N} \left\{ \frac{\partial H}{\partial \mathbf{r}_i} \cdot \frac{\partial}{\partial \mathbf{v}_i} - \frac{\partial H}{\partial \mathbf{v}_i} \cdot \frac{\partial}{\partial \mathbf{r}_i} \right\} = \hat{L}_0 + \delta \hat{L}. \tag{7}$$

Replacing H from Eq. (1) and with our choice of units we have

$$\hat{L}_0 = \sum_{i=1}^{s} \mathbf{v}_i \cdot \frac{\partial}{\partial \mathbf{r}_i}, \qquad \delta \hat{L} = \frac{1}{N} \sum_{i \neq j = 1}^{s} \frac{\partial V_{ij}}{\partial \mathbf{r}_i} \cdot \left(\frac{\partial}{\partial \mathbf{v}_i} - \frac{\partial}{\partial \mathbf{v}_j} \right). \tag{8}$$

A formal expression for the solution of the Liouville equation is given by [41]

$$f_N(t) = -\frac{1}{2\pi i} \oint dz\, e^{-izt} (\hat{L} - z)^{-1} f_N(0) = e^{-i\hat{L}_N t} f_N(0), \quad t > 0. \tag{9}$$

Using iteratively the identity

$$(\hat{L} - z)^{-1} \equiv (\hat{L}_0 - z)^{-1} [1 - \delta \hat{L} (\hat{L} - z)^{-1}] \tag{10}$$

results in a series solution of the Liouville equation:

$$|f_N(t)\rangle = -\frac{1}{2\pi i} \oint dz\, e^{-izt} \sum_{n=0}^{\infty} (\hat{L}_0 - z)^{-1} \times [-\delta \hat{L} (\hat{L}_0 - z)^{-1}]^n |f_N(0)\rangle, \tag{11}$$

where we introduced a Bra-Ket notation for the distribution function in phase space (see Ref. [16]). At this point it is important to note that the series expansion in Eq. (11) cannot be naively truncated at a given order of $\delta\hat{L}$, since the latter is of order N and thence each sum in Eq. (9) contributes a N factor. Nevertheless different contributions to the infinite series are grouped according to the diagrammatic representation in Appendix A. The higher order terms in $1/N$ can then be neglected consistently as we proceed to show.

Following the original approach by Balescu [42], we introduce the Fourier transform of the spatial dependence of f_s (the velocity dependence is left untouched) in d spatial dimensions, and the corresponding inverse transform:

$$
\begin{aligned}
&a_{\mathbf{k}_1,\ldots,\mathbf{k}_s}(\mathbf{v}_1,\ldots,\mathbf{v}_s,t)\\
&\quad=\int f_s(1,\ldots,s,t)\,\exp\left(i\sum_{j=1}^{s}\mathbf{k}_j\cdot\mathbf{r}_j\right)\,d\mathbf{r}_1\cdots d\mathbf{r}_s,\\
&f_s(1,\ldots,s,t)\\
&\quad=\frac{1}{[(2\pi)^d]^s}\int a_{\mathbf{k}_1,\ldots,\mathbf{k}_s}(\mathbf{v}_1,\ldots,\mathbf{v}_s)\\
&\qquad\times\exp\left(-i\sum_{j=1}^{s}\mathbf{k}_j\cdot\mathbf{r}_j\right)\,d\mathbf{k}_1\cdots d\mathbf{k}_s,
\end{aligned}
\tag{12}
$$

or equivalently

$$
\begin{aligned}
|f_s\rangle&=\sum_{\mathbf{k}_1,\ldots,\mathbf{k}_s}a_{\mathbf{k}_1,\ldots,\mathbf{k}_s}(\mathbf{v}_1,\ldots,\mathbf{v}_s,t)|\mathbf{k}_1,\ldots,\mathbf{k}_s\rangle,\\
a_{\mathbf{k}_1,\ldots,\mathbf{k}_s}(\mathbf{v}_1,\ldots,\mathbf{v}_s,t)&=\langle\mathbf{k}_1,\ldots,\mathbf{k}_s|f_s\rangle.
\end{aligned}
\tag{13}
$$

For some systems, as the ring model or the HMF model [14,15,38], the configuration space is periodic, and the Fourier transform is replaced by a Fourier series. By integrating Eq. (12) over particles 2 through N the only remaining contributions are those with at most one nonvanishing wave vector:

$$
f_1(\mathbf{r},\mathbf{v})=a_0(\mathbf{v},t)+\int a_{\mathbf{k}}(\mathbf{v},t)e^{-i\mathbf{k}\cdot\mathbf{r}}\,d\mathbf{k},
\tag{14}
$$

where we used the identity

$$
\int e^{i\mathbf{k}\cdot\mathbf{r}}\,d\mathbf{r}=(2\pi)^d\delta(\mathbf{k}),
\tag{15}
$$

with $\delta(\mathbf{k})$ the d-dimensional Dirac delta function. Therefore only the time evolution of coefficients with one or no nonvanishing wave vectors must be determined in order to obtain a kinetic equation. We explicitly obtain all diagrams contributing to the leading order in $1/N$ as follows. First, any possible diagram contributing to a_0 must start with a vertex of type C (see Fig. 16 in Appendix A), and it would necessarily act on the right on a Fourier coefficient describing a correlation, which is at most of order N^{-1}. Since we already have a N^{-1} factor from the vertex, for such a diagram to be independent of N we should sum over two particles (each sum contributing a factor N), but this would lead to vanishing surface terms. Therefore the diagram is at most of order $1/N$. Following this reasoning, adding more vertices to the diagram cannot result in a diagram independent of N. As a consequence

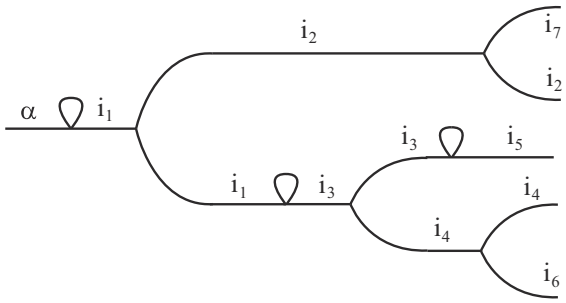

FIG. 1. Example of diagram occurring in Eq. (A4) contributing to the Fourier coefficient $a_{\mathbf{k}}$.

a_0 is constant in time up to this order. Similarly, the only nonvanishing contributions to $a_{\mathbf{k}}$ are diagrams formed by any combination of vertices of type D and F (Fig. 1 shows an example of such diagrams). All N dependencies are taken into account by considering the Kac factor $1/N$ in each vertex and a N factor for each sum over a particle index.

All diagrams contributing to $a_{\mathbf{k}}$ are put into two classes: those beginning at left with vertex F (class F) and those beginning with a vertex D (class D). Removing the first vertex F on the left in class F results in diagrams contributing to $a_{\mathbf{k}}(\mathbf{v}_j,t)$, and similarly removing the first vertex D on the left in class D gives those contributions to $a_{\mathbf{k}'}(\mathbf{v}_\alpha,t)a_{\mathbf{k}-\mathbf{k}'}(\mathbf{v}_j,t)$. Thence the formal solution has the following general structure:

$$
\begin{aligned}
a_{\mathbf{k}}(\mathbf{v}_\alpha,t)=&-\frac{1}{2\pi i}\oint e^{-izt}\,\frac{1}{i\,(\mathbf{k}\cdot\mathbf{v}_\alpha-z)}\\
&\times\left[a_{\mathbf{k}}(0)-\frac{i}{N}\sum_j V_{\mathbf{k}}\,\mathbf{k}\cdot\partial_{\alpha j}\,\mathcal{F}_{\mathbf{k}}\right.\\
&\left.-\frac{i}{N}\sum_j\int V_{|\mathbf{k}-\mathbf{k}'|}(\mathbf{k}-\mathbf{k}')\partial_{\alpha j}\mathcal{D}_{\mathbf{k}',\mathbf{k}-\mathbf{k}'}\,d\mathbf{k}'\right]dz,
\end{aligned}
\tag{16}
$$

where $\mathcal{D}_{\mathbf{k}',\mathbf{k}-\mathbf{k}'}$ and $\mathcal{F}_{\mathbf{k}}$ represent the contributions from class D and F above after removing the first vertex at its left in each diagram, respectively, and $\partial_{ij}=\partial/\partial v_i-\partial/\partial v_j$. Differentiating both sides with respect to time introduces a factor $-iz=i(\mathbf{k}\cdot\mathbf{v}_\alpha-z)-i\mathbf{k}\cdot\mathbf{v}_\alpha$ in the integrand, and yields after some manipulations:

$$
\begin{aligned}
&\frac{\partial}{\partial t}a_{\mathbf{k}}(\mathbf{v}_\alpha,t)\\
&\quad=-i\mathbf{k}\cdot\mathbf{v}_\alpha\,a_{\mathbf{k}}(\mathbf{v}_\alpha,t)+V_{\mathbf{k}}\,i\mathbf{k}\cdot\frac{\partial}{\partial\mathbf{v}_\alpha}\int a_{\mathbf{k}}(\mathbf{v}',t)\,d\mathbf{v}'\\
&\qquad+\frac{\partial}{\partial\mathbf{v}_\alpha}\cdot\int d\mathbf{k}\int d\mathbf{v}'\,i\,V_{|\mathbf{k}-\mathbf{k}'|}(\mathbf{k}-\mathbf{k}')a_{\mathbf{k}'}(\mathbf{v}_\alpha,t)a_{\mathbf{k}-\mathbf{k}'}(\mathbf{v}',t).
\end{aligned}
\tag{17}
$$

Using Eq. (14) and the results in Appendix A we finally obtain (after dropping out the index α):

$$
\begin{aligned}
\frac{\partial}{\partial t}f(\mathbf{r},\mathbf{v};t)=&-\mathbf{v}\cdot\frac{\partial}{\partial\mathbf{r}}f(\mathbf{r},\mathbf{v};t)+\frac{\partial}{\partial\mathbf{v}}f(\mathbf{r},\mathbf{v};t)\cdot\frac{\partial}{\partial\mathbf{r}}\\
&\times\int d\mathbf{r}'d\mathbf{v}'\,V(|\mathbf{r}-\mathbf{r}'|)f(\mathbf{r}',\mathbf{v}';t),
\end{aligned}
\tag{18}
$$

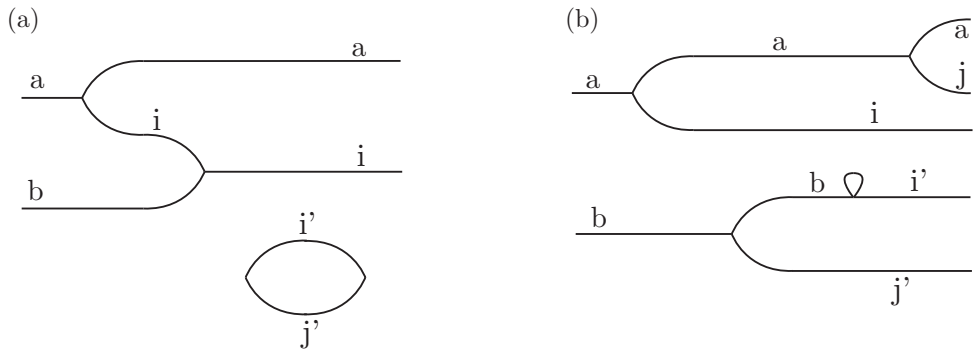

FIG. 2. Examples of diagram contributing to the coefficient $a_{\mathbf{k}_\alpha,\mathbf{k}_\beta}$.

where for simplicity we dropped the index in $f_1 \equiv f$. Equation (18) is the desired form for the Vlasov equation. It can also be obtained in the same way for a system of nonidentical self-gravitating particles as explained in Appendix B. In the next section we discuss how to consider the contributions of correlation (possibly) present in the initial state.

A. Order of magnitude of the correlations in N

Due to the linearity of the Liouville equation (6) and the linear dependence of f_N on the Fourier coefficients $a_{\{\mathbf{k}\}}(\mathbf{v},t)$ in Eq. (12) the order of magnitude of correlations for the initial distributions is kept constant by the time evolution. Therefore, if all correlations in the system are dynamically created, they are expected to have the same dependency on N as in the final state, i.e., the thermodynamical equilibrium (this point is discussed at length in Refs. [41,42]). It was shown in Ref. [40] that the microcanonical equilibrium distribution factorizes up to terms of order N^{-1}:

$$f_N^{\mathrm{eq}}(1,\ldots,N) = \prod_{i=1}^{N} f_1^{\mathrm{eq}}(\mathbf{r}_i,\mathbf{v}_i) + O\left(\frac{1}{N}\right). \tag{19}$$

The Fourier transform of the factorized equilibrium distribution function leads to

$$a^{\mathrm{eq}}_{\mathbf{k}_1,\ldots,\mathbf{k}_N}(\mathbf{v}_1,\ldots,\mathbf{v}_N) = \prod_{i=1}^{N} a^{\mathrm{eq}}_{1,\mathbf{k}_i}(\mathbf{v}_i) + O\left(\frac{1}{N}\right). \tag{20}$$

Therefore we assume that the correlation pattern $a_{[\mathbf{k}_1,\ldots,\mathbf{k}_l]}$ in Eq. (A1) is at least one order of magnitude less than the purely factored term $a_{\mathbf{k}_1}a_{\mathbf{k}_2}\cdots a_{\mathbf{k}_l}$. Figure 2 shows two examples of different contributions to the coefficient $a_{\mathbf{k}_\alpha,\mathbf{k}_\beta}$ with diagrams composed of four vertices of type A, B, C, and D contributing with a factor N^{-4}. From property 4 in Appendix A2, we see that in Fig. 2(a) either $j' = \alpha$ or $j' = \beta$ in order to yield a nonvanishing contribution, and three summations over particle indices: i, j and i', contributing with a factor N^3. The diagram is thus of order N^{-1}. A similar analysis for the diagram in Fig. 2(b) implies that it is independent of N (four vertices and four particle indices). Therefore in Fig. 2 diagram (a) is negligible while (b) must be retained. Diagram (a) creates a correlation among particles α and β while diagram (b) does not.

From these examples it is straightforward to see that only a succession of vertices of type D and F contributes to any reduced distribution function f_s, and therefore cannot create any correlations among particles 1 through s. This proves that the factorization of the distribution functions is maintained by the dynamics up to terms of order N^{-1}. More importantly, this result implies that, provided all correlations are created solely by the dynamics, the one-particle distribution function at any stage of the time evolution can be used as the initial condition for the Vlasov equation. Then from this new starting point slowly deviates from the finite N dynamics due to the cumulative secular effects of lower order collisional terms.

III. CONVERGENCE TO THE VLASOV LIMIT FOR SOME REPRESENTATIVE MODELS

In order to show how different interaction potentials lead to different convergence speed to the Vlasov (mean-field) dynamics we consider three different one-dimensional models with long-range interactions extensively studied in the literature: the Hamiltonian mean field model (HMF), with Hamiltonian [45]:

$$H = \frac{1}{2}\sum_{i=1}^{N} p_i^2 + \frac{1}{2N}\sum_{i,j=1}^{N}[1-\cos(\theta_i-\theta_j)], \tag{21}$$

where θ_i is the position angle of particle i and p_i its conjugate momentum, the ring model [14]:

$$H = \frac{1}{2}\sum_{i=1}^{N} p_i^2 - \frac{1}{2N}\sum_{i,j=1}^{N}\frac{1}{\sqrt{2}\sqrt{1-\cos(\theta_i-\theta_j)+\epsilon}}, \tag{22}$$

where ϵ is a softening parameter introduced to avoid the zero distance divergence in the pair interaction potential, and the infinite sheet model in three dimensions, describing N infinite planes with constant mass density and moving only along the x axis [39]:

$$H = \frac{1}{2}\sum_{i=1}^{N} p_i^2 + \frac{1}{2N}\sum_{i,j=1}^{N}|x_i - x_j|, \tag{23}$$

where x_i is ith particle coordinate. The Hamiltonian in Eq. (23) describes an effective one-dimensional model. We also consider a two-dimensional system with N identical particles with unit mass and unit gravitational constant with

Hamiltonian [8]:

$$H = \frac{1}{2}\sum_{i=1}^{N} \mathbf{p}_i^2 + \frac{1}{2N}\sum_{i,j=1}^{N} \log(|\mathbf{r}_{ij}| + \epsilon), \tag{24}$$

where $\mathbf{r}_{ij}$ is the vector from particle i to particle j and ϵ a softening parameter. The so-called Kac factor N^{-1} is again introduced with a change of time units (see Ref. [46] for a discussion of its interpretation and formal results valid for self-gravitating systems).

All simulations for the one-dimensional models were performed starting from a water-bag initial condition defined by

$$f_0(p,\theta) = \begin{cases} 1/(2p_0\theta_0), & \text{if } -p_0 < p < p_0 \text{ and } 0 < \theta < \theta_0, \\ 0, & \text{otherwise,} \end{cases} \tag{25}$$

for the HMF and ring models, and

$$f_0(p,x) = \begin{cases} 1/(4p_0x_0), & \text{if } -p_0 < p < p_0 \text{ and } -x_0 < x < x_0, \\ 0, & \text{otherwise,} \end{cases} \tag{26}$$

for the sheets model. Values chosen for p_0, θ_0 and x_0 are indicated in the respective figure captions. For the two-dimensional self-gravitating systems the initial distribution is given by all particles at rest and uniformly distributed in a circular shell of inner and outer radius R_1 and R_2, respectively, and commonly used in astrophysical simulations [47]. Molecular dynamics (MD) simulations were performed using a fourth-order simplectic integrator [48,49] for the HMF and ring models and an event-driven algorithm for the sheets model [50]. Time steps for simplectic integration are also indicated in the figure captions. All Vlasov simulations are performed using the approach described in Ref. [51] with a numerical grid with 4096×4096 points in the p,θ or p,x one-particle phase space. The force on particle i for the HMF model can be written as

$$F_i = M_y \cos\theta_i - M_x \sin\theta_i, \tag{27}$$

where the "magnetizations" components are given by

$$M_x = \frac{1}{N}\sum_{i=1}^{N} \cos\theta_i, \quad M_y = \frac{1}{N}\sum_{i=1}^{N} \sin\theta_i. \tag{28}$$

Since there are N forces to compute and the numerical effort to compute the magnetization components scales with N, the overall simulation time for MD simulations also scales with N, and thence simulations with a great number of particles are feasible. Figure 3 shows the kinetic energy for the HMF model obtained from the solution of the Vlasov equation and MD simulations with some different values of N, with a very good agreement already for $N = 10\,000$ up to $t \approx 20.0$. The time interval for which finite N and Vlasov solutions agree increases with N, as expected. Simulations for the ring model are shown in Fig. 4 for some values of the softening parameter ϵ. Convergence toward the Vlasov values for the kinetic energy gets clearly slower for smaller ϵ, as the interaction gets stronger at short distances where collisional effects are more important. For the self-gravitating sheets model, an increasing agreement with increasing N is also obtained as given in Fig. 5.

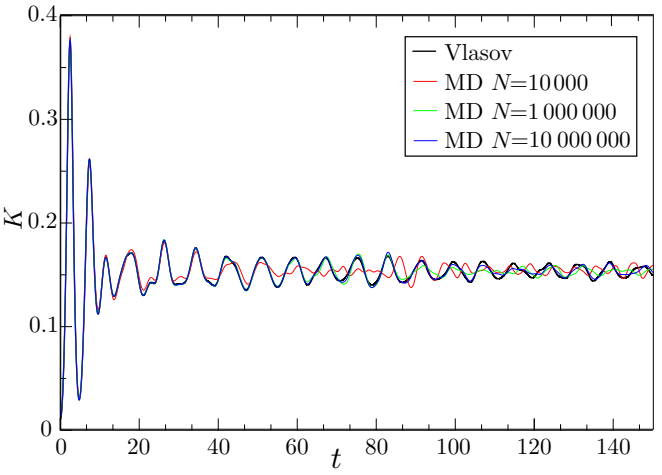

FIG. 3. (Color online) Kinetic energy for Vlasov and MD simulations for the HMF model as a function of time. Initial conditions as given in Eq. (25) with $p_0 = 0.25$ and $\theta_0 = 4.0$. Time steps are $\Delta t = 0.01$ for Vlasov simulation and $\Delta t = 0.1$ for MD simulations.

Although the results obtained here are qualitative, they point to the fact that the convergence to a mean-field description is thus strongly affected by the values of the force at short distance. The stronger that the latter the more important are the collisional effects, and the smaller is the agreement time window of the Vlasov equation with the finite N dynamics.

IV. EVOLUTION OF INTERPARTICLE CORRELATIONS WITH TIME

Even though the Vlasov equation can be deduced from the BBGKY hierarchy by imposing uncorrelated particles, i.e., a fully factored N-particle distribution function, the results in Sec. II stress the fact that the order of magnitude of the correlations are preserved by the dynamics and, provided all interparticle correlations are dynamically created (see also Ref. [42]), that the Vlasov equation is valid at any stage of the evolution with an error of order $1/N$ by considering the one-particle distribution function at this given time as the initial condition for the Vlasov equation. From this point on, its solution will secularly deviate from the distribution function for finite N due to collisional terms of order $1/N$ or lower (see Sec. V). In order to illustrate this point, let us consider the HMF model with a homogeneous (water bag) initial condition. To measure interparticle correlations we remember that the central limit theorem states that the distribution of a sum of n identical uncorrelated random variables x_i of the form

$$X^{(n)} = \sum_{i=1}^{n} x_i \tag{29}$$

converges to a Gaussian distribution in the $n \to \infty$ limit. A simple and straightforward measure (among others) of the deviation from the distribution of $X^{(n)}$ to a Gaussian is given

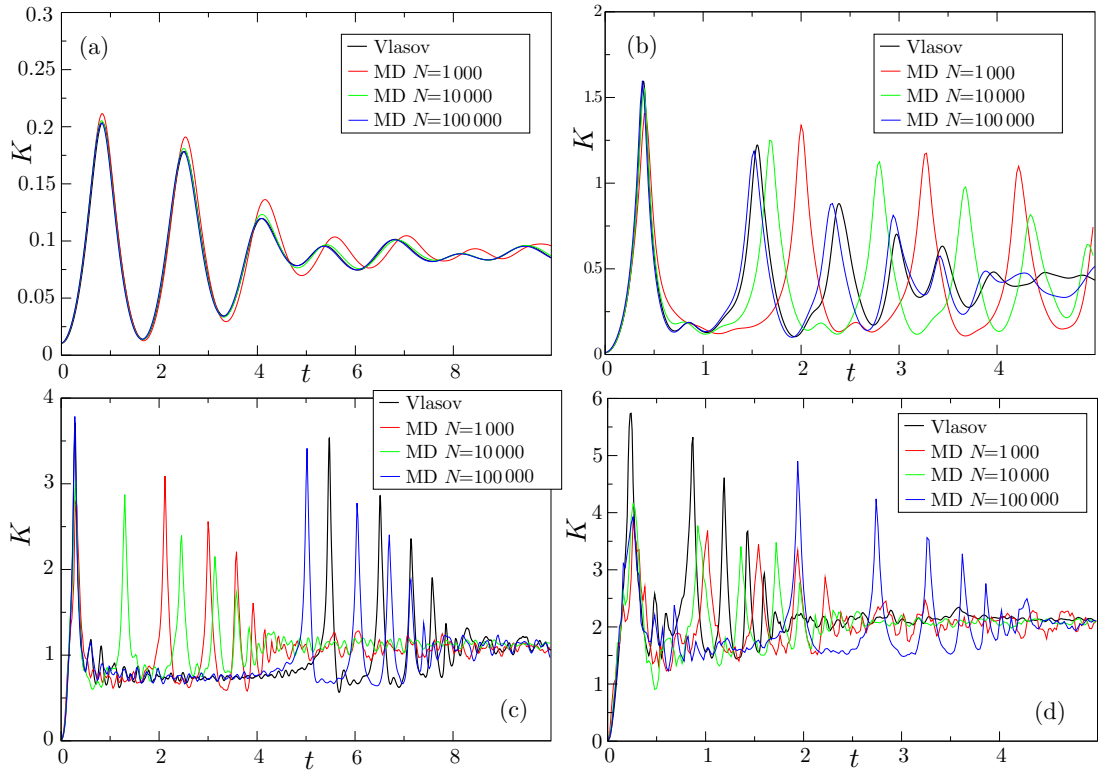

FIG. 4. (Color online) Kinetic energy for Vlasov and MD simulations for the ring model with $\epsilon = 10^{-1}$ (a), $\epsilon = 10^{-2}$ (b), $\epsilon = 10^{-3}$ (c), $\epsilon = 10^{-4}$ (d). The initial condition is a water-bag state with $p_0 = 0.25$ and $\theta_0 = 1.0$. Time steps for Vlasov and MD simulations are $\Delta t = 10^{-3}$.

by its kurtosis:

$$\mathcal{K} = \left\langle \frac{(X^{(n)} - \langle X^{(n)} \rangle)^4}{\sigma_X^4} \right\rangle, \tag{30}$$

where $\langle \cdots \rangle$ define the ensemble average and σ_X the standard deviation of $X^{(n)}$. For all Gaussian distributions the kurtosis as defined in Eq. (30) has the value $\mathcal{K} = 3$ and is very sensitive to any deviation from the Gaussian and converges to this value as $1/n$ for uncorrelated identical variables. For a correlated variable the distribution either does not converge to a Gaussian (and therefore a different value for the Kurtosis) or converges very slowly, requiring that one sum a very large number n of random variables to approach a Gaussian distribution (see Ref. [52] and references therein). This method is particularly useful as the corresponding computer implementation scales with the number of elements in the realization instead to its square as for other correlation measures. This is particularly important here to not spoil the optimizations in simulations for the HMF model (that scale linearly with N). For a realization with a finite number of random numbers drawn from a uniform distribution the kurtosis will fluctuate around the exact value $\mathcal{K} = 3$. The greater the realization, the closest it will be to this value. As an illustration of this point the kurtosis for 100 and 10 000 realizations of the sum of $M = 256$ random numbers obtained from a good random number generator [43] as a function of n is shown in Fig. 6. Note that fluctuations around the Gaussian value are always present for a finite realization and decrease with increasing number of realizations N_r. In what follows the value of N_r is limited for a given number N

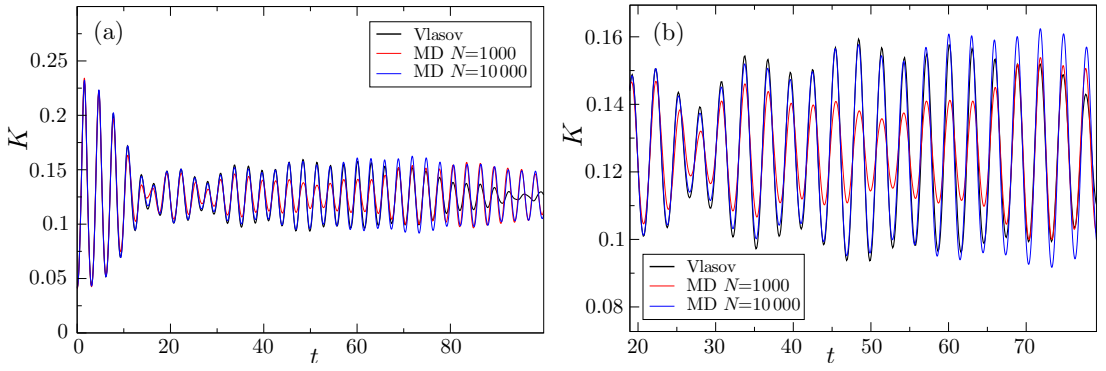

FIG. 5. (Color online) (a) Kinetic energy for Vlasov and MD simulations for the self-gravitating sheets model with Hamiltonian in Eq. (23). (b) A zoom over a region where the MD simulation deviates significantly from the Vlasov solution.

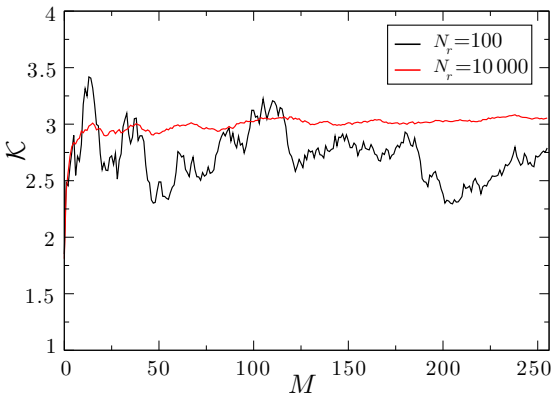

FIG. 6. (Color online) Kurtosis for a sum of M (uncorrelated) random number variables for $1 \leqslant M \leqslant 256$, with $N_r = 100$ and $N_r = 10\,000$ realizations.

of particles to $N_r = N/256$. In the results below we always use the value $M = 256$ for computational convenience.

In this way we measure interparticle correlations by partitioning the set of all N particles into N/M groups with M particles each (we suppose N is divisible by M or just discard the data for the few remaining particles). Then we define the variables for $k = 1, \ldots, N_r = N/M$:

$$y_k = \sum_{i=1}^{M} \theta_{(k-1)M+i}, \qquad z_k = \sum_{i=1}^{M} p_{(k-1)M+i}, \tag{31}$$

and the reduced variables

$$\tilde{y}_k = (y_k - \langle y \rangle)/\sigma_y, \qquad \tilde{z}_k = (z_k - \langle z \rangle)/\sigma_z, \tag{32}$$

where $\langle \cdots \rangle$ stands for the statistical average and σ_y and σ_z are the standard deviations of y and z, respectively. If particles are uncorrelated the central limit theorem states that the distribution of y_k and z_k tends rapidly to a Gaussian with increasing M. Figure 7 shows the kinetic and potential energies per particle for a simulation of the HMF model with $N = 262\,144$ particles and a homogeneous initial water-bag state with total energy per particle $E = 0.5879$, such that the initial state is stable but close to the instability threshold (see Sec. V). The crossover from the homogeneous water-bag state to the final thermodynamical equilibrium is clearly visible. Figure 8 shows the kurtosis $\mathcal{K}_p$ and $\mathcal{K}_\theta$ for the variables $\tilde{y}$ and $\tilde{z}$ with $M = 256$ along the time evolution including the destabilization of the water-bag state for some increasing values of N. Both kurtoses tend to the exact Gaussian value at all instants of times as N increases, for two reasons: first, correlations among particles become increasingly small as the mean-field description becomes closer to the true dynamics, and second, the number of realization N_r of the summed variables also increases. A more pronounced variation is seen in the initial stage of the evolution corresponding to the violent relaxation [44], but even there it tends to the Gaussian values as N increases.

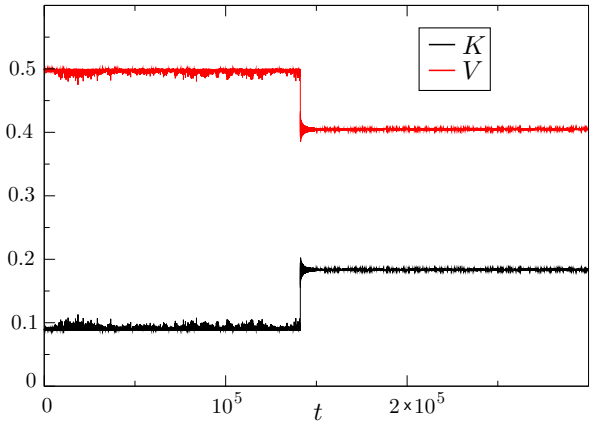

FIG. 7. (Color online) Kinetic K and potential V energies per particles for the HMF model with $N = 262\,144$ particles water-bag initial condition with $p_0 = 0.726$ and $\theta_0 = 2\pi$, corresponding to zero initial magnetization and total energy per particle $E = 0.5879$, $\Delta t = 0.5$.

Figure 9 shows the same kurtosis $\mathcal{K}_p$ and $\mathcal{K}_\theta$ but for a much longer simulation time for $N = 100\,000$ such that the final equilibrium state is attained at the end of the simulation. As expected some deviations from the value corresponding to uncorrelated particles is observed, but with a constant amplitude indicating that once interparticle correlations are created, their order of magnitude is conserved during all of the time evolution, in accordance with the analytical analysis in Sec. II. Indeed, $\mathcal{K}_p$ and $\mathcal{K}_\theta$ oscillate around the value 3 for all times.

Following the same reasoning we present now simulations for the two-dimensional self-gravitating system with Hamiltonian given in Eq. (24). Figure 10 shows the time evolution of potential and kinetic energies with $N = 16\,384$ particles, $R_1 = 1.0$, $R_2 = 1.5$, $\epsilon = 10^{-4}$, and all particles initially at rest. The violent relaxation is clearly visible, with the final state close to the Gaussian equilibrium. Figure 11 shows the kurtosis $\mathcal{K}_r$ and $\mathcal{K}_v$ of the corresponding reduced variables in Eq. (32) for the x components of the position $\mathbf{r}$ and velocity $\mathbf{v}$, respectively, with $M = 256$ for $N = 16\,384$ and $N = 131\,072$. Again correlations are created, but the amplitude of oscillation of $\mathcal{K}_v$ and $\mathcal{K}_r$ is essentially the same all along the time evolution and decreases as N increases, again in agreement with the statement in Sec. II that interparticle correlations maintain their order of magnitude with N.

V. QUASISTATIONARY STATES AND VLASOV INSTABILITY

Quasistationary states of the N-particle dynamics of long-range interacting systems are now identified with stable stationary solutions of the Vlasov dynamics [2] with a finite lifetime due to the loss of stability of the solution of the Vlasov equation from the slow secular evolution of the one-particle distribution function. Indeed, as at any considered time the Vlasov equation gives an accurate description of the dynamics up to terms of order N^{-1} (provided all interparticle correlations

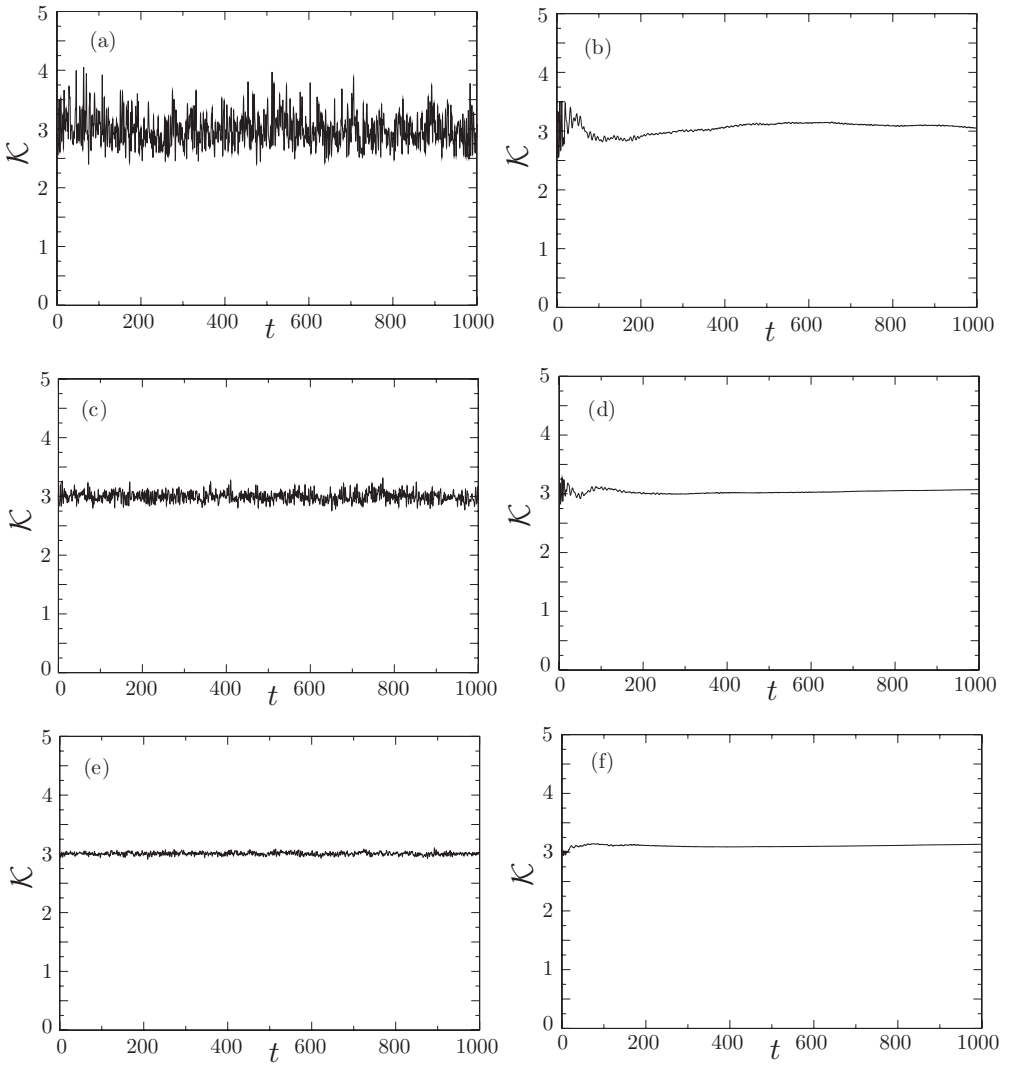

FIG. 8. Kurtosis for the variables in Eq. (32) for the HMF model corresponding to the same initial condition as in Fig. 7. (a), (c), and (e) kurtosis $\mathcal{K}_p$ for the sum of momenta variables for $N = 100\,000$, $N = 1\,000\,000$, and $N = 10\,000\,000$, respectively. (b), (d), and (e) kurtosis $\mathcal{K}_\theta$ for the sum of position variables corresponding to the panels at its left. The value $M = 256$ is used in Eq. (31) for all cases.

are dynamically generated), it is valid to consider as an initial condition for the Vlasov equation the distribution at any given time, and therefore the stability of the slowly varying state is dictated by the Vlasov equation. In Ref. [33] it was shown for the HMF model that a homogeneous QSS with one-particle momentum distribution function $f(p)$ is stable if the following

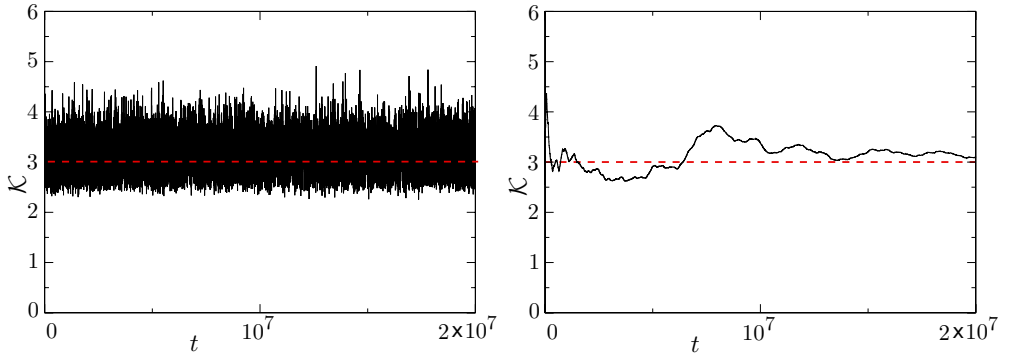

FIG. 9. (Color online) Kurtosis for the variables in Eq. (32) for the HMF model and corresponding to the same initial condition as in in Fig. 7 with $N = 100\,000$ and $M = 256$ but for a total simulation time $t_f = 2.0 \times 10^7$ such that the system is at thermodynamic equilibrium at the end of the simulation. (a) Kurtosis for the sum of momenta variables. (b) Kurtosis for the sum of position variables. The dashed line is used for reference and is set at the Gaussian value $\mathcal{K} = 3$.

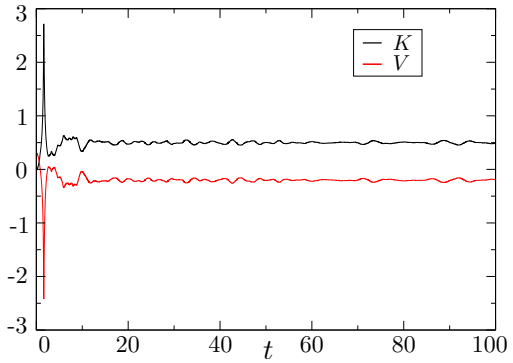

FIG. 10. (Color online) Kinetic (K) and potential (V) energies per particle for as a function of time for the two-dimensional self-gravitating system with $N = 131\,072$ particles, $R_1 = 1.0$, $R_2 = 1.5$, and $\epsilon = 10^{-4}$ with all particles initially at rest.

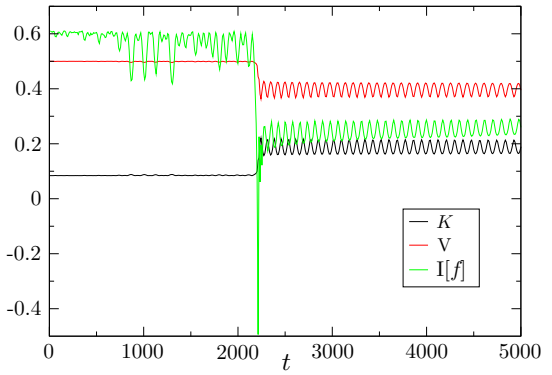

FIG. 12. (Color online) Kinetic and potential energies and stability parameter $I[f]$ as defined in Eq. 33, for a homogeneous water-bag initial distribution, $p_0 = 0.355$ and $N = 10\,000\,000$.

condition is satisfied:

$$I[f] \equiv 1 + \frac{1}{2}\int_{-\infty}^{\infty} \frac{f'(p)}{p}\, dp > 0. \tag{33}$$

From the considerations above, the lifetime of a homogeneous QSS is given by the value of time at which $I[f]$ becomes negative, as a result of the cumulative effects of collisions (graininess), irrespective of the presence of any correlations created from collisions or the time elapsed since the (uncorrelated) initial state. This is illustrated in a simulation with $N = 10\,000\,000$ particles in Fig. 12. The time value at which the QSS looses its stability is also precisely the moment at which $I[f]$ in Eq. (33) becomes negative.

Even though the QSS has a finite lifetime due to small collisional terms, the state after the loss of stability can still be used as an initial condition for the Vlasov equation to describe the time evolution of the system for another finite time span. As an example we consider a MD simulation with the same initial condition as in Fig. 12 but with $N = 1\,048\,576$ particles and stopped just after the loss of stability of the QSS. Then the one-particle distribution function is determined from simulated data and used as the initial state for a Vlasov simulation. The left panel in Fig. 13 shows the results for the kinetic energy for both Vlasov and MD simulations starting from this same initial state, and both agree quite well.

For finite N a QSS is continually changing with time due to the cumulative effects of collisions. A lifetime can be

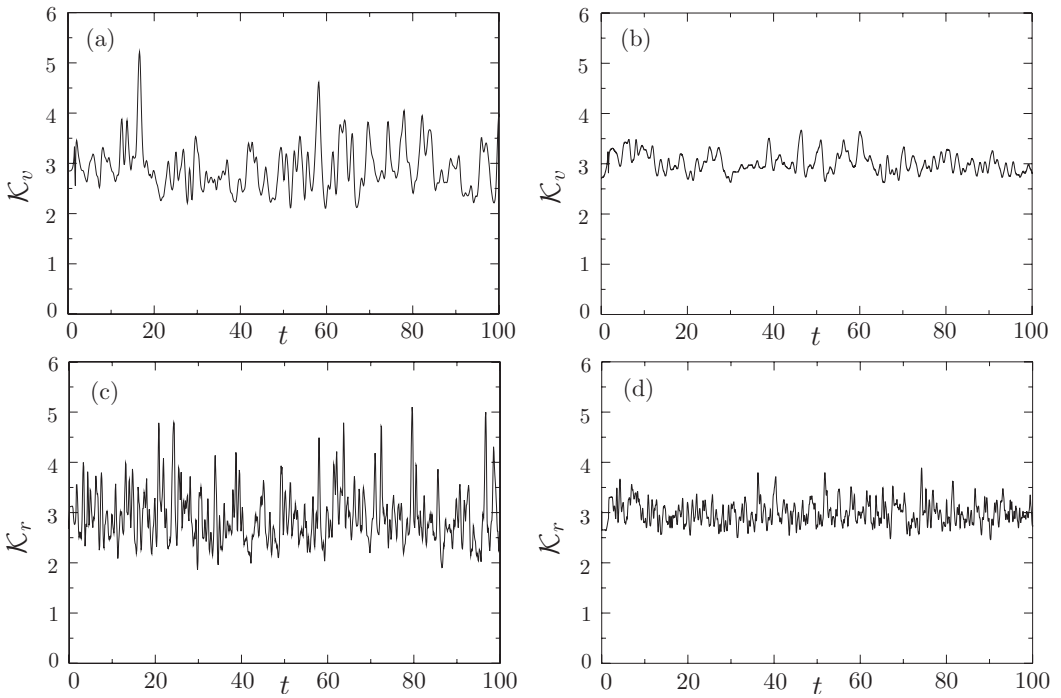

FIG. 11. Kurtosis for the same initial condition as in Fig. 10 with $N = 16\,384$ for panels (a) $\mathcal{K}_v$ and (c) K_r, and 131 072 for panels (b) $\mathcal{K}_v$ and (d) K_r, respectively, and $M = 256$.

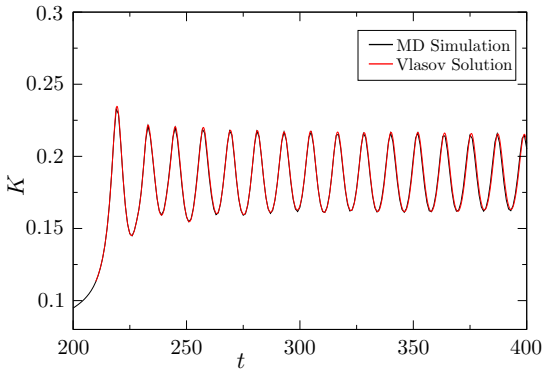

FIG. 13. (Color online) Same as in Fig. 12 but $N = 1\,048\,576$ and the Vlasov simulation stating from the distribution function obtained from the final state of a MD simulation at $t = 210$. Both oscillate at almost the same frequency, with a slight shift as time evolves, and are very close to one another.

meaningfully ascribed only if a given property of the state changes abruptly, as, for instance, in the case corresponding to Fig. 12 where the magnetization changes from a vanishing value associated with a homogeneous state to a nonvanishing value. Nevertheless this abrupt change or dynamical phase transition [21] is due to the loss of Vlasov stability of the homogeneous QSS. These changes do not always occur, and as an example let us consider the HMF model with a three-level distribution initial condition given by

$$f_0(p,\theta) = \begin{cases} f_1 & \text{if } |p| \leqslant p_1 \text{ and } 0 < \theta < \theta_0, \\ f_2 & \text{if } p_1 < |p| < p_2 \text{ and } 0 < \theta < \theta_0, \\ 0 & \text{otherwise,} \end{cases} \tag{34}$$

for p_1, p_2, f_1 and f_2 given constants. Figure 14(a) shows the kinetic and potential energies per particle for a choice of these constants. The nonhomogeneous state resulting from the violent relaxation is stable (this is shown if the figure where increasing values of N lead to slower variation of K and V), but effects of collisions are nevertheless pronounced, in such a way that it is hardly possible to consider this state as quasistationary. Figure 14(b) shows that the collisional evolution after the violent relaxation scales with N as expected since in this case the kinetic equation is given by the Landau or Balescu-Lenard equations with a collisional integral proportional to N. For homogeneous states the picture changes as can be seen in Fig. 14(c). Since the kinetic and potential energies are almost constant for the time interval considered, the slow secular evolution of the velocity distribution function is better grasped by considering its first moments $M_k = \langle p^k \rangle$. Moments M_4 and M_6 are shown in Fig. 14(d) with the cumulative effects of collisions clearly visible. As discussed in the introduction the Landau and Balescu-Lenard collisional integrals vanish

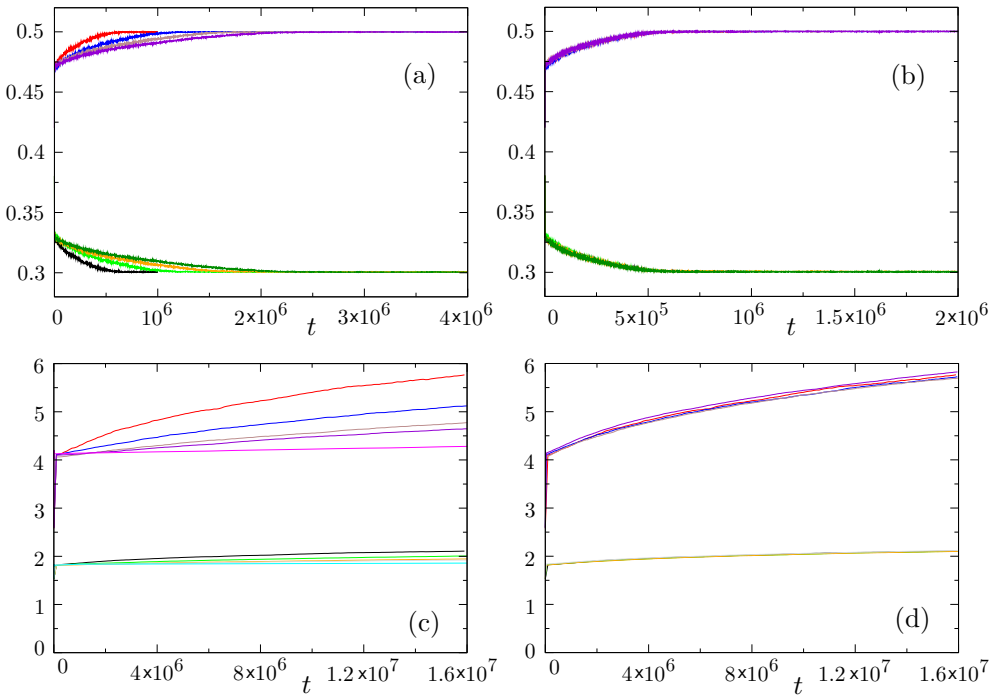

FIG. 14. (Color online) (a) Evolution of kinetic K (upper curves) and potential V (lower curves) energies per particle for the three level initial condition in Eq. (34) with $p_1 = 0.3$, $p_2 = 1.8$, $f_1 = 0.0454$, $f_2 = 0.165$, $\theta_0 = 4.25$ corresponding for the values $N = 100\,000$, $N = 200\,000$, $N = 300\,000$, and $N = 400\,000$. The greater the value of N the greater the time to attain the plateaus in the curves. (b) Same as (a) but with a rescaling of time $t \to t/(N \times 10^{-3})$ as expected for a nonhomogeneous state. (c) Fourth (lower curves) and sixth (upper curves) moments of the velocity distribution function for a three-level initial condition with $p_1 = 0.3$, $p_2 = 1.8$, $f_1 = 0.061$, $f_2 = 0.041$, $\theta_0 = 2\pi$ and for $N = 40\,000$, $N = 60\,000$, $N = 80\,000$, $N = 100\,000$, and $N = 200\,000$. The greater N the smaller the derivative of the moments at a given time. (d) Same as (c) but with a time rescaling $t/(N/40\,000)^2$. All curves collapse in a single curve for each moment.

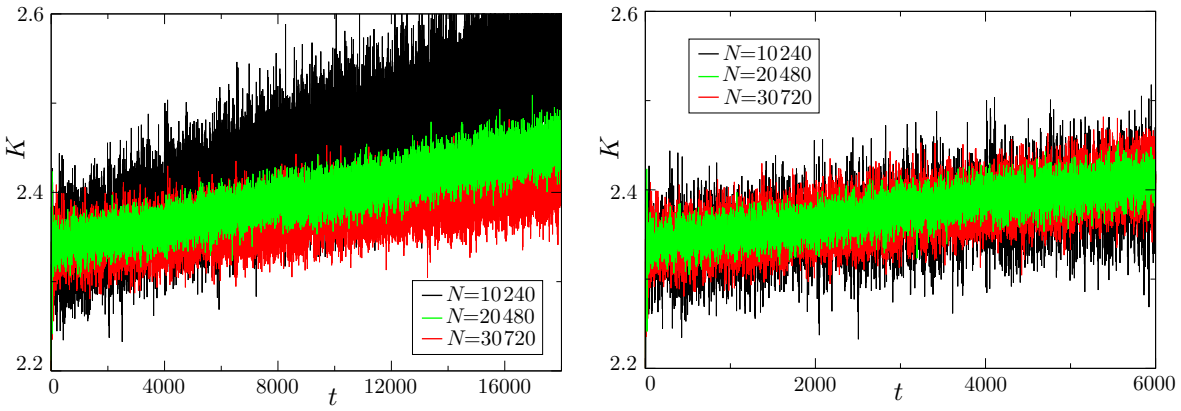

FIG. 15. (Color online) Left: Kurtosis $\mathcal{K} = \langle v_x^4 \rangle / \langle v_x^2 \rangle^2$ of the x component of the velocity distribution function as a function of time for the two-dimensional self-gravitating system with Hamiltonian in Eq. (24), with a virialized initial condition and a spatially uniform distribution on a disk with unit radius, for different number of particles. Right: The same as the left panel but with a rescaling of time $t \to t/(N/10\,240)$.

in the homogeneous states of one-dimensional systems, and consequently the scaling of the time evolution with N must be slower than for the inhomogeneous case. Fig. 14(d) shows the same curves but with a rescaling proportional to N^2, resulting in a data collapse for all curves. This as important result since it is at variance with the $N^{1.7}$ and e^N scalings obtained in Refs. [19,20], respectively, but is in agreement with the same scaling obtained for homogeneous one-dimensional plasmas in Refs. [36,37]. For inhomogeneous states and higher dimensional systems this scaling is predicted from well-established physical theories, such as for the result shown in Fig. 15 for the two-dimensional self-gravitating system where a scaling proportional to N is evident, in accordance with the results in Ref. [53] but at variance with those in Ref. [8].

There are some possibilities to explain those different scalings in the time evolution for the homogeneous states of the HMF model. Either the scaling is state dependent since in our case we considered a three-level initial state, while in Refs. [19,37] a water-bag and semielliptic initial distributions were used, respectively. This would imply that the N dependence of the collisional integral in the still unknown kinetic equation would vary with the statistical state, which in the authors' opinion would be a quite awkward case. Another possible explanation would be that since the author of Refs. [19,37] considered only small numbers of particles in their simulations (20 000 at the most) and much smaller than the cases considered here, the $N^{1.7}$ and e^N scaling would be due to the small size of their systems. A separate publication will thoroughly explore such possibilities and discuss how to obtain a kinetic equation valid for homogeneous states of one-dimensional systems [54].

VI. CONCLUDING REMARKS

In order to show how different interaction potentials lead to different convergence speeds to the Vlasov (mean-field) dynamics we have considered three different one-dimensional models with long-range interactions extensively studied in the literature: the Hamiltonian mean-field model (HMF) and the self-gravitating ring and self-gravitating sheets models. All simulations for these models were performed starting from a water-bag initial condition indicated in Eqs. (25) and (26). The validity of the mean-field description was assessed by comparing the results from MD simulations for different particle numbers to numerical solutions of the Vlasov equation.

Simulations for the ring model are shown in Fig. 4 for some values of the softening parameter ϵ. Convergence towards the values for the kinetic energy obtained from direct numerical solutions of the Vlasov equation gets clearly poorer for smaller values of this parameter, as the interaction gets stronger at short distances where collisional effects are more important. For the self-gravitating sheet model, an increasing agreement with increasing N is also obtained as shown in Fig. 5. The convergence to a mean-field description is thus strongly affected by the force at short distances. The stronger the latter, the more important are the collisional effects, and the smaller the time window during which the particle dynamics agrees with the Vlasov equation within small errors of order $1/N$.

For sake of completeness and for the present paper to be self-contained, we discuss in the appendices the derivation of the Vlasov equation from a resummation of different contributions of a diagrammatic expansion using the Kac factor $1/N$ as the relevant small parameter. It is shown that provided all interparticle correlations are dynamically created, they do not alter the validity of the Vlasov equation, since their order of magnitude in N is preserved by the dynamics as seen from the results and discussion in Secs. II and IV. This means that deviations from the solution of the Vlasov equation are not due to an increase in correlations with time, but to the secular accumulation of small collisional corrections of order $1/N$ (see Sec. IV). Again, although correlations are always present, they contribute to the kinetic equation only at order $1/N$ (or lower). The one-particle distribution function at any point of the evolution can thus be used as the initial condition to solve the Vlasov equation, which is valid for a given time span starting at this specific value of time.

We also obtained a scaling proportional to N^2 for the dynamics of a homogeneous state of the HMF model, at variance with previous results that used a smaller number of particles than in the present work [19,20]. For a two-dimensional system we obtained a scaling in agreement with

Ref. [53] but at variance with Ref. [8]. This is a clear indication that a more comprehensive study of this problem is still lacking and is the subject of a separate publication [54].

ACKNOWLEDGMENTS

This work is partially financed by CNPq and CAPES (Brazilian government agencies).

APPENDIX A: KINETIC EQUATION FOR LARGE N: THE VLASOV EQUATION

Here we show that the one-particle distribution function of long-range interacting systems satisfies the Vlasov equation for a large number of particles N. The approach chosen here, i.e., the dynamics of correlations, is fully developed in Balescu's monograph [42] (see Ref. [16] for the notations used in this paper) and essentially follows the same steps used in the original derivation by Balescu, but instead of the plasma constant we use here $1/N$ as a small parameter for the diagram selection leading to the Vlasov equation. This is an alternative proof of the validity of the Vlasov equation for the one-particle reduced distribution function for long-range interacting systems in the $N \to \infty$ limit. This approach is succinctly present here, and its extension for self-gravitating systems of nonidentical particles is discussed in Appendix B.

1. Formal solution of the Liouville equation

A generic Fourier coefficient as defined in Eq. (12) can be decomposed as

$$a_{\mathbf{k}_1,\ldots,\mathbf{k}_l} = a_{\mathbf{k}_1} a_{\mathbf{k}_2} \cdots a_{\mathbf{k}_l} + a_{[\mathbf{k}_1,\ldots,\mathbf{k}_l]}, \tag{A1}$$

as a sum of a completely factored part and a pure correlation represented by $a_{[\mathbf{k}_1,\ldots,\mathbf{k}_l]}$. The completeness relation for the Fourier basis is given by

$$\frac{1}{2\pi^{dN}} \int \exp\left(-i \sum_{j=1}^{N} \mathbf{k}_j \cdot \mathbf{r}_j\right) \exp\left(i \sum_{j=1}^{N} \mathbf{k}_j \cdot \mathbf{r}'_j\right) = \delta\left[\sum_{j=1}^{N} (\mathbf{r}_k - \mathbf{r}'_j)\right], \tag{A2}$$

or equivalently in the more concise Bra-Ket notation:

$$\int |\{\mathbf{k}\}\rangle\langle\{\mathbf{k}\}| \, d^N\mathbf{k} = \hat{\mathbf{I}}, \tag{A3}$$

where $\{\mathbf{k}\} \equiv \mathbf{k}_1, \ldots, \mathbf{k}_N$. Using Eq. (11) we obtain

$$\begin{aligned} a_{\{\mathbf{k}\}}(\mathbf{v},t) &= \langle\{\mathbf{k}\}| f_N(t)\rangle \\ &= -\frac{1}{2\pi i} \oint dz\, e^{-izt} \left[R_{\mathbf{k}}(z)\, \delta^{Kr}(\{\mathbf{k} - \mathbf{k}'\}) \right. \\ &\quad - R_{\mathbf{k}}(z)\, \langle\{\mathbf{k}\}|\delta\hat{L}|\{\mathbf{k}'\}\rangle\, R_{\mathbf{k}'}(z) \\ &\quad + \sum_{\{\mathbf{k}''\}} R_{\mathbf{k}}(z) \langle\{\mathbf{k}\}|\delta\hat{L}|\{\mathbf{k}''\}\rangle\, R_{\mathbf{k}''}(z) \\ &\quad \left. \times \langle\{\mathbf{k}''\}|\delta\hat{L}|\{\mathbf{k}'\}\rangle\, R_{\mathbf{k}'}(z) + \cdots \right] a_{\{\mathbf{k}'\}}(\mathbf{v},0), \end{aligned} \tag{A4}$$

with

$$R_{\mathbf{k}}(z) = i \left[z - \sum_{j=1}^{N} \mathbf{k}_j \cdot \mathbf{v}_j \right]^{-1}, \tag{A5}$$

$$\langle\{\mathbf{k}\}|\delta\hat{L}|\{\mathbf{k}'\}\rangle = \sum_{j<l} \delta L_{jl}(\{\mathbf{k}\},\{\mathbf{k}'\}),$$

$$\delta L_{jl}(\{\mathbf{k}\},\{\mathbf{k}'\}) = -\frac{i}{N} V_{|k_j - k'_j|}(\mathbf{k}_j - \mathbf{k}'_j)\, \partial_{jl} \delta(\mathbf{k}_j + \mathbf{k}_l - \mathbf{k}'_j - \mathbf{k}'_l) \prod_{m \neq j,l} \delta^{Kr}(\mathbf{k}_m - \mathbf{k}'_m), \tag{A6}$$

where $\delta^{Kr}(\{\mathbf{k}\}) = \prod_j \delta^{Kr}(\mathbf{k}_j)$, $\delta^{Kr}(0) = 1$, $\delta^{Kr}(\mathbf{k} \neq 0) = 0$ and the Fourier transform of the potential given by

$$V_k = \int V(r) e^{i\mathbf{k}\cdot\mathbf{r}}\, dr. \tag{A7}$$

Note that V_k depends only on $k = |\mathbf{k}|$ for a central potential.

2. Diagrammatic representation

Each term in the expansion (A4) can be represented by a diagram according to the following rules:

(1) For each element $R_{\mathbf{k}}(z)$ we associate a set of lines going from right to left. The number of lines are the same as the number of nonvanishing wave vectors in the set $\{\mathbf{k}\}$;

(2) Each line has an index that represents the particle associated to the wave vector.

(3) To each term $\delta L_{ij}(\{\mathbf{k}\},\{\mathbf{k}'\})$ we associate a vertex, with in and out lines concurrent with those with index i and n in the set $\{\mathbf{k}\}$ (if exists) and one of lines with index j and n in the set $\{\mathbf{k}'\}$ (if exists).

(4) When considering the contribution to the reduced distribution f_s, for each vertex at least one of its two particles index must belong to the set $\{1, \ldots, s\}$ or appear at a line at its left.

Rule 4 comes from the presence of the operator ∂_{ij} in the definition of δL in Eq. (A6), leading to a vanishing surface term if this rule is not satisfied.

From Eq. (A6) the wave vectors change only two by two such that $\mathbf{k}_1 + \mathbf{k}_2 = \mathbf{k}'_1 + \mathbf{k}'_2$. In this way there are six possible vertices as shown in Fig. 16. To each line to the left and to the

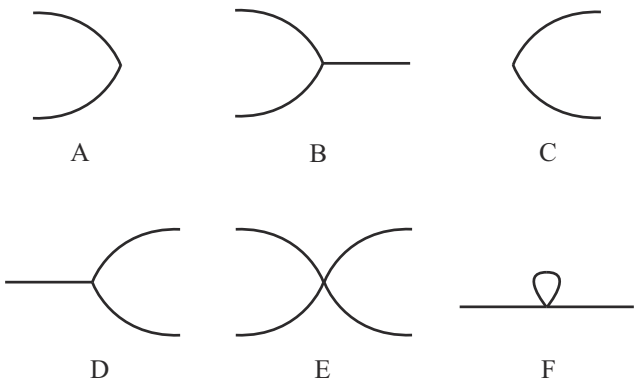

FIG. 16. Different vertices representing the interaction term in Eq. (A6).

right of a vertex we associate a particle index. Some examples of diagrams are given in Fig. 2.

In the arguments of a Fourier coefficient we write explicitly only the velocities of those particles with a nonvanishing wave vector, and for the Fourier coefficient of s-particle distribution functions a vanishing wave vector for a given particle implies an integration over the coordinates (but not the velocities) of this particle.

APPENDIX B: SYSTEMS WITH NONIDENTICAL PARTICLES: SELF-GRAVITATING SYSTEMS

For nonidentical particles the N-particle distribution function f_N is not symmetric, and the above approach cannot be used as such. Let us consider now a subset of s particles denoted by $\{i_k\} \equiv \{i_1, \ldots, i_s\}$, with each i_k different from the other particle indices in the set and ranging from 1 to N. The s-particle distribution function for the set $\{i_k\}$ is defined by

$$f_s(\{i_k\}) \equiv f_s(i_1, \ldots, i_s) = \int f_N(1, \ldots, N)\, dj_1 \cdots dj_{N-s}, \tag{B1}$$

where $\{j_l\}$ is the set of particle indices from the N-particle set not contained in $\{i_k\}$. By integrating both sides of Eq. (6) over the coordinates and momenta of particles in $\{j_l\}$, and discarding surface terms, we obtain

$$\left[\frac{\partial}{\partial t} - \hat{L}_s\right] f_s(\{i_k\}) = \sum_{k=1}^{s} \sum_{l=1}^{N-s} \frac{\partial}{\partial \mathbf{p}_{i_k}} \cdot \int \frac{\partial V_{i_k j_l}}{\partial \mathbf{r}_{i_k}} f_{s+1}(\{i_k\}, j_l)\, dj_l, \tag{B2}$$

where $\hat{L}_s$ is the Liouville operator for the s-particle subsystem and $f_{s+1}(\{i_k\}, j_l)$ stands for $f_{s+1}(i_1, \ldots, i_s, j_l)$. At this point it is important to notice that since we are considering the possibility of a system with different masses, the reduced functions as defined by Eq. (B1) are not symmetric by permutation of two particles and Eq. (B2) is the final form of the BBGKY hierarchy.

For a self-gravitating system of particles with different masses, the potential energy is written as

$$V_{ij} = V(|\mathbf{r}_i - \mathbf{r}_j|) = -G m_i m_j \frac{\mathbf{r}_i - \mathbf{r}_j}{|\mathbf{r}_i - \mathbf{r}_j|^3} \equiv m_i m_j h(\mathbf{r}_i - \mathbf{r}_j), \tag{B3}$$

where $h(\mathbf{r}_i - \mathbf{r}_j)$ is the force between two particles of unit mass at positions $\mathbf{r}_i$ and $\mathbf{r}_j$. This particular form can be used to further simplify the hierarchy in Eq. (B2). To illustrate how to proceed we consider the case $s = 1$. We first define the one-particle mass density in phase space:

$$F_1(\mathbf{r}, \mathbf{p}) = \sum_{i=1}^{N} m_i f_1^{(i)}(\mathbf{r}, \mathbf{p}), \tag{B4}$$

where $f_1^{(i)}(\mathbf{r}, \mathbf{p})$ is given by $f_1(\mathbf{r}_i, \mathbf{p}_i)$ computed at $\mathbf{r}_i = \mathbf{r}$ and $\mathbf{p}_i = \mathbf{p}$. Similarly we define

$$F_2(\mathbf{r}, \mathbf{p}, \mathbf{r}', \mathbf{p}') = \sum_{i \neq j = 1}^{N} m_i m_j f_2(i, j) \Big|_{i = \mathbf{r}, \mathbf{p}, : j = \mathbf{r}', \mathbf{p}'}, \tag{B5}$$

which as defined is symmetric by permutation of $\mathbf{r}, \mathbf{p}$ and $\mathbf{r}', \mathbf{p}'$. Using Eq. (B2) for $s = 1$ and Eqs. (B4) and (B5), it is straightforward to show that

$$\left[\frac{\partial}{\partial t} + \mathbf{v} \cdot \frac{\partial}{\partial \mathbf{r}}\right] F_1(\mathbf{r}, \mathbf{p}) = -\frac{\partial}{\partial \mathbf{v}} \cdot \int \mathbf{h}(\mathbf{r} - \mathbf{r}') F_2(\mathbf{r}, \mathbf{p}, \mathbf{r}', \mathbf{p}')\, d\mathbf{r}\, d\mathbf{p}. \tag{B6}$$

A similar simplification is not possible for $s \geqslant 3$ due to the operator $\hat{L}_s$ in the left-hand side of Eq. (B2). From the discussion above on identical particles, it is reasonable to suppose that correlations between particles are of order N^{-1} and therefore negligible for large N. For a system of self-gravitating identical particles this statement can be proved using the diagrammatic method along the same lines as for a plasma [42].

[1] A. Campa, T. Dauxois, and S. Ruffo, Phys. Rep. **480**, 57 (2009).

[2] T. Dauxois, S. Ruffo, E. Arimondo, and M. Wilkens (eds.), *Dynamics and Thermodynamics of Systems with Long-Range Interactions* (Springer, Berlin, 2002).

[3] A. Campa, A. Giansanti, G. Morigi, and F. S. Labini (eds.), *Dynamics and Thermodynamics of Systems with Long-Range Interactions: Theory and Experiments* (AIP, New York, 2008), AIP Conf. Proceedings Vol. 970 (2008).

[4] T. Dauxois, S. Ruffo, and L. F. Cugliandolo (eds.), *Long-Range Interacting Systems, Les Houches 2008, Session XC* (Oxford University Press, Oxford, 2010).

[5] T. M. Rocha Filho, A. Figueiredo, and M. A. Amato, Phys. Rev. Lett. **95**, 190601 (2005).

[6] A. Figueiredo, T. M. Rocha Filho, and M. A. Amato, Europhys. Lett. **83**, 30011 (2008).

[7] T. Padmanabhan, Phys. Rep. **188**, 285 (1990).

[8] T. N. Teles, Y. Levin, R. Pakter, and F. B. Rizzato, J. Stat. Mech. (2010) P05007.

[9] Y. Levin, R. Pakter, and T. N. Teles, Phys. Rev. Lett. **100**, 040604 (2008).

[10] F. B. Rizzato, R. Pakter, and Y. Levin, Phys. Rev. E **80**, 021109 (2009).

[11] B. E. Turkington, in *Long-Range Interacting Systems, Les Houches 2008, Session XC*, edited by T. Dauxois, S. Ruffo, and L. F. Cugliandolo (Oxford University Press, Oxford, 2010), Chap. 4.

[12] J. Barré, T. Dauxois, G. De Ninno, D. Fanelli, and S. Ruffo, Phys. Rev. E **69**, 045501(R) (2004).

[13] P. de Buyl, D. Fanelli, R. Bachelard, and G. De Ninno, Phys. Rev. ST Accel. Beams **12**, 060704 (2009).

[14] Y. Sota, O. Iguchi, M. Morikawa, T. Tatekawa, and K. I. Maeda, Phys. Rev. E **64**, 056133 (2001).

[15] T. Tatekawa, F. Bouchet, T. Dauxois, and S. Ruffo, Phys. Rev. E **71**, 056111 (2005).
[16] R. L. Liboff, *Kinetic Theory: Classical, Quantum and Relativistic Descriptions*, 3rd ed. (Springer, New York, 2003).
[17] M. Kac, G. Uhlenbeck, and P. Hemmer, J. Mathy. Phys. **4**, 216 (1963).
[18] W. Braun and K. Hepp, Commun. Math. Phys. **56**, 101 (1977).
[19] Y. Yoshiyuki, Y. Yamaguchi, J. Barré, F. Bouchet, T. Dauxous, and S. Ruffo, Phys. A **337**, 36 (2004).
[20] A. Campa, A. Giansanti, and G. Morelli, Phys. Rev. E **76**, 041117 (2007).
[21] A. Campa, P. H. Chavanis, A. Giansanti, and G. Morelli, Phys. Rev. E **78**, 040102(R) (2008).
[22] M. Joyce and T. Worrakitpoonpon, J. Stat. Mech. (2010) P10012.
[23] S. Gupta and D. Mukamel, J. Stat. Mech. (2010) P08026.
[24] S. Gupta and D. Mukamel, J. Stat. Mech. (2011) P03015.
[25] S. Gupta and D. Mukamel, Phys. Rev. Lett. **105**, 040602 (2010).
[26] P. de Buyl, D. Mukamel, and S. Ruffo, Phys. Rev. E **84**, 061151 (2011).
[27] T. N. Teles, Y. Levin, R. Pakter, and F. B. Rizzato, J. Stat. Mech. (2010) P05007.
[28] P. H. Chavanis, J. Stat. Mech. (2010) P05019.
[29] P. H. Chavanis, Eur. Phys. J. Plus **127**, 19 (2012).
[30] P. H. Chavanis, arXiv:1303.0998 [cond-mat.stat-mech].
[31] P. H. Chavanis, arXiv:1303.1004 [cond-mat.stat-mech].
[32] M. M. Sano, J. Phys. Soc. Jpn. **81**, 024008 (2012).
[33] Y. Y. Yamaguchi, J. Barré, F. Bouchet, T. Dauxois, and S. Ruffo, Phys. A **337**, 36 (2004).
[34] F. Bouchet and T. Dauxois, Phys. Rev. E **72**, 045103(R) (2005).
[35] P. H. Chavanis, Phys. A **387**, 787 (2008).
[36] J. Dawson, Phys. Fluids **7**, 419 (1964).
[37] J. L. Rouet and M. R. Feix, Phys. Fluids B **3**, 1830 (1991).
[38] M. Antoni and S. Ruffo, Phys. Rev. E **52**, 2361 (1995).
[39] K. R. Yawn and B. N. Miller, Phys. Rev. E **68**, 056120 (2003).
[40] P.-H. Chavanis, Physica A **361**, 55 (2006).
[41] R. Balescu, *Statistical Mechanics: Matter Out of Equilibrium* (Imperial College Press, London, 1997).
[42] R. Balescu, *Statistical Dynamics of Charged Particles* (Interscience, London, 1963).
[43] D. E. Knuth, *The Art of Computer Programmins*, Vol. 2 (Addison Wesley, Reading, 1998).
[44] D. Lynden-Bell, Mon. Not. R. Astr. Soc. **136**, 101 (1967).
[45] M. Antoni and S. Ruffo, Phys. Rev. E **52**, 2361 (1995).
[46] M. K. H. Kiessling, J. Stat. Phys. **55**, 203 (1989).
[47] I. Arad and D. Lynden-Bell, Mon. Not. R. Astr. Soc. **361**, 385 (2005).
[48] H. Yoshida, Phys. Lett. A **150**, 262 (1990).
[49] T. M. Rocha Filho, arXiv:1212.0262 [physics.comp-ph].
[50] D. C. Rapaport, *The Art of Molecular Dynamcs Simulation*, 2nd ed. (Cambridge University Press, Cambridge, 2004).
[51] T. M. Rocha Filho, Comp. Phys. Comm. **184**, 34 (2013).
[52] A. Figueiredo, I. Gléria, R. Matsushita, and S. D. Silva, Phys. Lett. **326**, 166 (2004).
[53] B. Marcos, arXiv:1212.0959 [cond-mat.stat-mech].
[54] T. M. Rocha Filho, A. Figueiredo, A. E. Santana, and M. A. Amato, arXiv:1305.4417 [cond-mat].